Research Article
Experimental and Translational Hepatology

JOURNAL
OF HEPATOLOGY

MicroRNA-27a-3p targets FoxO signalling to induce tumour-like phenotypes in bile duct cells

Authors

Lea Duwe, **Patricia Munoz-Garrido**, Monika Lewinska, …, Jill Koshiol, Colm J. O'Rourke, Jesper B. Andersen

Correspondence

jesper.andersen@bric.ku.dk (J.B. Andersen).

Graphical abstract

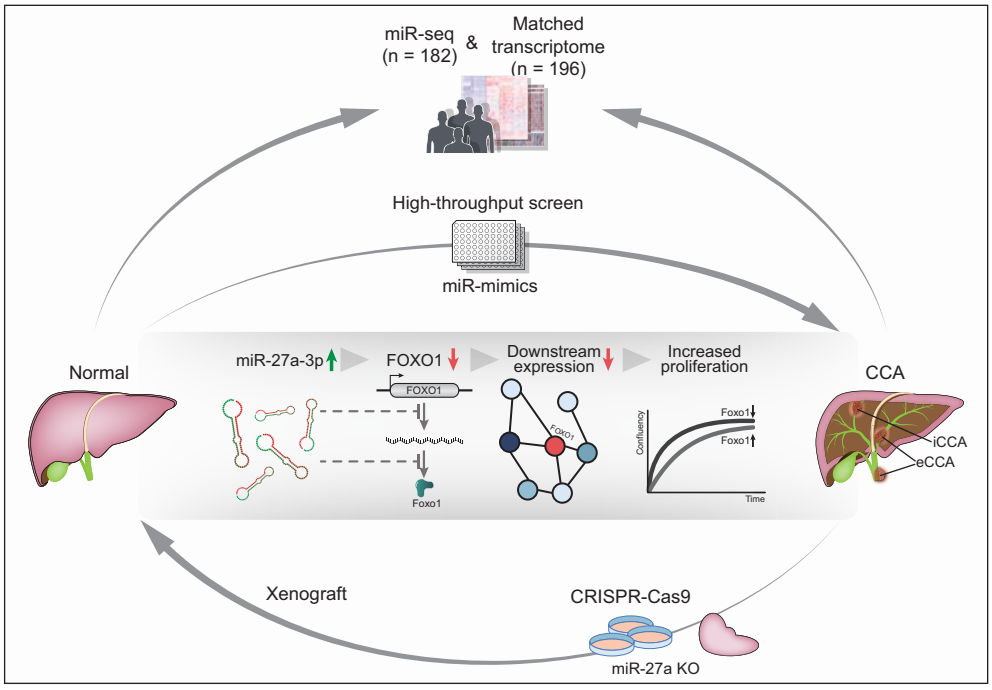

Highlights

- CCA tissues are characterized by miR upregulation, increased miR biogenesis pathway expression and miR heterogeneity.
- Most miRs upregulated in CCA resulted in increased proliferation when introduced into human cholangiocyte models *in vitro.*
- MiR-27a-3p affects FoxO signalling in individuals with CCA *in vitro* and *in vivo.*
- CRISPR/Cas9 nickase knockout of miR-27a abrogates tumorigenicity *in vitro* and *in vivo.*

Impact and implications

Cholangiocarcinogenesis entails extensive cellular reprogramming driven by genetic and non-genetic alterations, but the functional roles of these non-genetic events remain poorly understood. By unveiling global miRNA upregulation in patient tumours and their functional ability to increase proliferation of cholangiocytes, these small non-coding RNAs are implicated as critical non-genetic alterations promoting biliary tumour initiation. These findings identify possible mechanisms for transcriptome rewiring during transformation, with potential implications for patient stratification.

https://doi.org/10.1016/j.jhep.2022.10.012
 J. Hepatol. 2023, 78, 364–375

Research Article
Experimental and Translational Hepatology

JOURNAL
OF HEPATOLOGY

MicroRNA-27a-3p targets FoxO signalling to induce tumour-like phenotypes in bile duct cells

Lea Duwe[1,†], **Patricia Munoz-Garrido**[1,†], Monika Lewinska[1], Juan Lafuente-Barquero[1], Letizia Satriano[1], Dan Høgdall[1,2], Andrzej Taranta[1], Boye S. Nielsen[3], Awaisa Ghazal[1], Matthias S. Matter[4], Jesus M. Banales[5,6,7,8], Blanca I. Aldana[9], Yu-Tang Gao[10], Jens U. Marquardt[11], Lewis R. Roberts[12], Rui C. Oliveira[13,14], Jill Koshiol[15], Colm J. O'Rourke[1], Jesper B. Andersen[1,*]

Journal of Hepatology **2023**. vol. 78 | 364–375

Background & Aims: Cholangiocarcinoma (CCA) is a heterogeneous and lethal malignancy, the molecular origins of which remain poorly understood. MicroRNAs (miRs) target diverse signalling pathways, functioning as potent epigenetic regulators of transcriptional output. We aimed to characterise miRNome dysregulation in CCA, including its impact on transcriptome homeostasis and cell behaviour.

Methods: Small RNA sequencing was performed on 119 resected CCAs, 63 surrounding liver tissues, and 22 normal livers. High-throughput miR mimic screens were performed in three primary human cholangiocyte cultures. Integration of patient transcriptomes and miRseq together with miR screening data identified an oncogenic miR for characterization. MiR-mRNA interactions were investigated by a luciferase assay. MiR-CRISPR knockout cells were generated and phenotypically characterized *in vitro* (proliferation, migration, colony, mitochondrial function, glycolysis) and *in vivo* using subcutaneous xenografts.

Results: In total, 13% (140/1,049) of detected miRs were differentially expressed between CCA and surrounding liver tissues, including 135 that were upregulated in tumours. CCA tissues were characterised by higher miRNome heterogeneity and miR biogenesis pathway expression. Unsupervised hierarchical clustering of tumour miRNomes identified three subgroups, including distal CCA-enriched and *IDH1* mutant-enriched subgroups. High-throughput screening of miR mimics uncovered 71 miRs that consistently increased proliferation of three primary cholangiocyte models and were upregulated in CCA tissues regardless of anatomical location, among which only miR-27a-3p had consistently increased expression and activity in several cohorts. FoxO signalling was predominantly downregulated by miR-27a-3p in CCA, partially through targeting of *FOXO1*. MiR-27a knockout increased FOXO1 levels *in vitro* and *in vivo*, impeding tumour behaviour and growth.

Conclusions: The miRNomes of CCA tissues are highly remodelled, impacting transcriptome homeostasis in part through regulation of transcription factors like *FOXO1*. MiR-27a-3p arises as an oncogenic vulnerability in CCA.

Introduction

Cholangiocarcinoma (CCA) is the second most-common primary liver cancer, encompassing a diverse group of malignancies arising in the intrahepatic or extrahepatic bile ducts, the latter being further divided in perihilar and distal CCA. Most patients diagnosed with CCA have sporadic disease, with no clear underlying risk factors.[1] While the underlying aetiologies of most tumours remain unknown,[2] chronic inflammation is believed to be causative of or at least contributory to cholangiocarcinogenesis.[3] The inflammatory environment triggers ductular reactions, involving hyperproliferation of cholangiocytes in response to immune stimuli. Rapid proliferation of cells in pro-inflammatory microenvironments is accompanied by epigenetic alterations, which lead to further genetic and epigenetic alterations, ultimately resulting in malignant transformation.[4] While genomic analysis of invasive CCA has identified clinically impactful DNA-based alterations in patients,[5–7] mutation rates are intermediate compared to other cancers[8] and are not alone sufficient to explain the major transcriptomic changes and complex biology exhibited by tumour cells. Of note, both mutations and different tumour aetiologies are linked to epigenetic changes in CCA,[7,9] but the contribution of epigenetic alterations to disease initiation remains poorly defined. Identifying epigenetic mechanisms that contribute to cholangiocarcinogenesis is fundamental to understanding disease risk and preventative management, as well as potentially expanding the repertoire of therapeutic targets beyond those identified from DNA sequence analysis.[10]

MicroRNAs (miRs) are small non-coding RNAs and key epigenetic regulators of the transcriptome. Their ability to

Keywords: Cholangiocarcinoma; cholangiocytes; FoxO1; microRNAs; proliferation.
Received 29 March 2022; received in revised form 7 October 2022; accepted 10 October 2022; available online 28 October 2022
* Corresponding authors. Address: Biotech Research and Innovation Centre (BRIC), Department of Health and Medical Sciences, University of Copenhagen, Denmark; Tel.: (+45) 35325834.
E-mail address: jesper.andersen@bric.ku.dk (J.B. Andersen).
† Equal author contribution
https://doi.org/10.1016/j.jhep.2022.10.012

regulate multiple transcripts enables extensive, rapid, and reversible transcriptomic regulation in response to external stimuli such as inflammation.[11] In CCA, miRs are involved in several oncogenic hallmarks, such as uncontrolled proliferation, decreased apoptosis, invasion and metastasis, and inflammation.[12] In particular, oncomiR miR-21 has been extensively studied in CCA. By regulating several key signalling pathways such as PI3K/AKT, ERK,[13] and PTEN,[14] miR-21 expression leads to increased epithelial-mesenchymal transition[13] and drug resistance.[15] It is therefore essential to perform larger scale analysis to be able to fully decipher the deregulated landscape of miRs and determine their impact on regulatory pathways involved in the development and progression of the disease.

In this study, we characterized the miRNomes and matched transcriptomes of CCA and surrounding liver (SL) tissues, and in parallel tested the ability of over 2,700 miR mimics to induce proliferation in normal human cholangiocytes. From these data, we identified miR-27a-3p as a critical pro-proliferative miR in patient tumours. This miR was implicated predominantly in the regulation of forkhead box O family (FoxO) signalling, in part by targeting *FoxO1*. The regulation of FOXO1 by miR-27a was subsequently confirmed to be oncogenic in CCA.

Materials and methods

Patient cohort and patient-derived models

Tissue samples were obtained from 128 treatment-naïve patients undergoing surgical resection with curative intent as part of their clinical management, including 63 matched-SL specimens. In total, 9 samples did not pass quality control during pre-processing. These samples were retrospectively identified from six clinical centers in Europe, the USA, and China. Additionally, 22 normal human liver samples were included as independent controls. These samples were obtained from the Liver Tissue Cell Distribution System at University of Pittsburgh (MTA36479-13). Patient consent and ethical approval were obtained for use of all samples and information evaluated in this study, in accordance with local, national, and international regulations (declaration of Helsinki).[7,16] These involved the Danish Committee system on Health and Research Ethics (Protocol no. H-4-2015-FSP; 15014207) as well as the NCI and Shanghai Cancer Institute (Shanghai Biliary Tract Cancer Case-control study, protocol no. OH97CN028). Patient consent and ethical approval were provided for the generation of primary patient-derived models[17] (no. 837.199.10 (7208), University of Mainz, Germany).

Small RNA sequencing and analysis

Total RNA was extracted from fresh-frozen resected tissues using AllPrep DNA/RNA/miRNA Universal Kit (Qiagen) following the manufacturer's protocol. RNA was quantified with Qubit RNA HS Assay Kit (Life Technologies) and RNA integrity number was determined in the Aligent 2100 Bioanalyzer System (RNA 6000 Nano Assay) according to the manufacturer's instructions, with a value >7 representing high-quality RNA. All samples were processed for small RNA sequencing (RNAseq) using the Hiseq 4000 system (Illumina) by Beijing Genomics Institute (BGI, https://www.bgi.com/global/, Copenhagen, DK), with a required coverage of >20 million matched reads. The data were subsequently processed by standardized bioinformatic pipelines.

High-throughput miR mimic screening

Three primary cultures of normal human cholangiocytes (C324, NHC2, NHC3)[18,19] were used for *in vitro* studies. Transfection of a human miR mimic library (based on miRBase Version 21, Sanger Institute) was performed in NHC3. The library consisted of 2,754 miR mimics (MISSION® microRNA Mimic, MI00300, Sigma-Aldrich). Briefly, NHC3 cells were reverse transfected in 384 well-plates with a final concentration of 10 nM of each miR mimic (in triplicates) using a Hamilton Microlab STARlet robot. MiR mimics were transiently transfected using Lipofectamine RNAiMAX (Life Technologies) according to the manufacturer's guidelines. Monitoring of cell proliferation changes were measured over time (0 to 120 h) using the real-time, non-invasive, and quantitative IncuCyte® Live-Cell Analysis System (ESSEN BIOSCIENCE). miR scrambles were used as transfection controls and taurocholic acid was used as a positive proliferation control. For further confirmation of our screening results, two validation screens were performed under the same conditions in NHC2 and C324.

Statistical analyses

For bioinformatics approaches, all analyses were conducted in R v4.0. Categorical data were compared between groups using Pearson's Chi-squared test with Yates' continuity correction or Fisher's exact test. For continuous data, normality was evaluated by Shapiro-Wilk test. Non-normally distributed data were compared and correlated using Wilcoxon rank-sum test with continuity correction and Spearman correlation, respectively. Normally distributed data were compared and correlated using Welch's *t* test and Pearson correlation. Heatmaps and correlation plots were generated using the 'gplots' and 'ggplot2' packages, respectively. Experimental results were statistically analysed using the GraphPad Prism 9 statistical software (San Diego, USA). All data are shown as mean ± standard deviation. For comparisons between two groups, a parametric unpaired *t* test or a non-parametric Mann-Whitney test were used. Differences were considered significant when $p < 0.05$.

For further details regarding the materials and methods used, please refer to the CTAT table and supplementary information.

Results

MiRNome aberrations are characteristic of CCA and implicated in tumour heterogeneity

High-quality small RNAseq data were generated for 119 CCA and 63 SL samples obtained during surgical resection. This cohort is comprised of patients enrolled from multiple clinical centres, overlapping with our previously reported transcriptome cohorts.[16,20] Clinicopathologic characteristics are summarized in Table S1. In total, 1,049 miRNAs were identified with a median mapped read count of 33,531,719 reads (range: 13,274,065-63,983,783) mapping to known miRs per sample (Table S2).

Comparing the miRNomes of CCA and SL samples using two independent methods (DESeq2; Wilcoxon rank-sum test of counts per million values), 140 differentially expressed miRs (DEmiRs; 135 higher and 5 lower expressed in CCA) were

identified by both methods (Table S3). Hierarchical clustering with the 140 DEmiRs significantly stratified the samples into tumour-associated and non-tumour-associated clusters (p <0.0001, chi-squared; Fig. 1A). The expression profile of these miRs appeared highly similar between SL and independent normal liver samples (n = 22), but 85.7% (120/140) of these DEmiRs were differentially expressed between tumour anatomical subtypes (Table S3). Among DEmiRs, 30.7% (43/

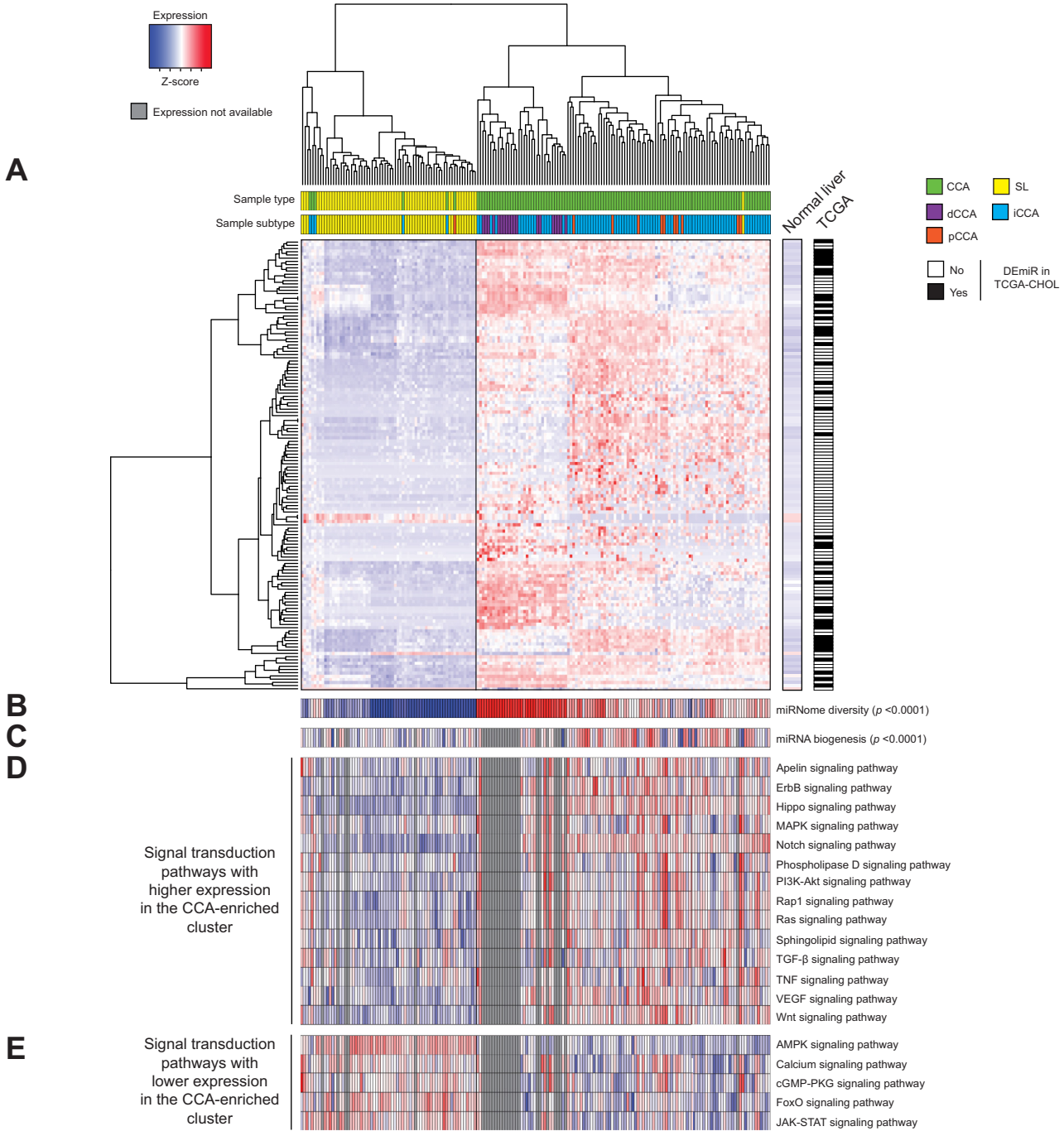

Fig. 1. Integrative small RNA sequencing and transcriptome analysis of CCA. (A) Supervised hierarchical clustering of CCA (n = 119) and SL (n = 63) samples with a heatmap of 140 DEmiRs. MiRs were only categorized as DEmiRs between CCA and SL samples, if they were identified by DESeq2 and Wilcoxon rank-sum test of normalized counts per million values. Relative mean expression of these DEmiRs in 22 independent normal liver samples is visualized in the 'Normal Liver' track. Differential expression analysis of the 140 DEmiRs in CCA (n = 36) and SL (n = 9) samples from TCGA-CHOL cohort is indicated in the 'TCGA' track. (B) Diversity of miR expression across samples, quantified using Simpson's diversity index. p values were calculated by Wilcoxon rank-sum test. (C) Expression of the miR biogenesis pathway (defined by Reactome) across samples, quantified using ssGSEA. p values were calculated by Wilcoxon rank-sum test. (D-E) Expression of signal transduction pathways (defined by KEGG) that are higher (D) or lower (E) in the tumour-associated cluster, quantified using ssGSEA. p values were <0.05 and calculated by Wilcoxon rank-sum test. CCA, cholangiocarcinoma; dCCA, distal CCA; DEmiRs, differentially expressed miRs; iCCA, intrahepatic CCA; miR, microRNA; pCCA, perihilar CCA; SL, surrounding liver; ssGSEA, single sample gene set enrichment analysis; TCGA, The Cancer Genome Atlas. (This figure appears in color on the web.)

140) were found to be reproducibly differentially expressed in The Cancer Genome Atlas (TCGA)-CHOL cohort. The CCA-associated cluster was characterized by higher intrasample miRNA diversity (p <0.0001, Wilcoxon rank-sum test of Simpson's diversity index; Fig. 1B) and higher miRNA biogenesis pathway expression (p <0.0001; Fig. 1C). A majority (58.3%, 14/24) of signalling pathways were more highly expressed in the CCA-associated cluster compared to SL, including common oncogenic networks (Apelin, ErbB, Hippo, MAPK, Notch, phospholipase D, PI3K-Akt, Rap1, Ras, Sphingolipid, TGF-B, TNF, VEGF and Wnt) (Fig. 1D, Table S4). In contrast, 20.8% (5/24) of signal transduction pathways were more lowly expressed in the CCA-associated cluster and included pathways associated with metabolic and immune regulation (AMPK, calcium, cGMP-PKG, FoxO, JAK-STAT) (Fig. 1E). As most DEmiRs are upregulated in tumours (96.4%, 135/140), resulting in negative regulation of their target genes, their major impact in CCA is likely through downregulation of critical pathways.

Unsupervised hierarchical clustering of CCA samples alone identified three miR expression-based clusters (Fig. S1A). Patient age did not differ between clusters (Table S5). While miR biogenesis pathway expression did not significantly differ between tumour clusters (p = 0.595, ANOVA), miR diversity was higher among cluster 2 tumours (p <0.0001, Wilcoxon; Fig.S1B). Using transcriptome-based deconvolution of cell types, no significant differences in fibroblast (p = 0.97, ANOVA) or immune cell (p = 0.25) content were identified between clusters (Fig.S1C). Cluster 1 (25.2%; 30/119) tumours were characterized by lower expression of ErbB (p = 0.0002), Hippo (p = 0.0027), Notch (p = 0.02), phospholipase D (p <0.03), sphingolipid (p = 0.0073) and Wnt (p = 0.0018) signalling pathways (Fig.S1D). Cluster 2 tumours (28.6%; 34/119) were enriched in distal CCA (p <0.0001, Fisher's exact test), Chinese origin (p <0.0001) and exhibited higher calcium signalling pathway expression (p = 0.03). Cluster 3 tumours (46.2%; 55/119) were associated with high expression of ErbB (p <0.04), Hippo (p = 0.0081), sphingolipid (p = 0.04) and Wnt (p <0.0090) signalling pathways, as well as lower calcium signalling pathway expression (p <0.03). Further, cluster 3 tumours were found to be enriched in females (p = 0.0138, Fisher's exact test) and *IDH1* mutations (p = 0.0045), whereas no significant association was found between other recurrent genomic alterations (mutations in *KRAS* or *TP53*, *FGFR2*:*BICC1* fusions) and tumour clusters (Fig.S1E, Table S6). Overall survival of patients differed between miR clusters (p = 0.0005, log-rank test), with cluster 2 patients exhibiting the shortest survival (Fig.S1F). Whole miRNome survival analysis identified 19 survival-associated miRs in individuals with resected CCA, independent of tumour location (multivariable Cox proportional hazards model, false discovery rate [FDR] p <0.05), as anatomical subtypes are associated with different survival outcomes for patients receiving best supportive care[2] (Fig.S1G, Table S7). Collectively, these data implicate miRs in diverse features of patient heterogeneity, such as tumour location, tumour genotype and pathobiological signalling, but independent from miRNA biogenesis pathway expression or tumour tissue composition.

High-throughput mimic screening in normal cholangiocytes identifies patient-relevant proliferative miRs

In parallel with miR profiling of resected CCA tissues, a high-throughput screen of 2,754 miR mimics was performed in normal human cholangiocytes (NHC3) to systematically identify miRs that increase cell proliferation (Fig. 2A, Fig. S2A). In total, 548 miRs were found to increase proliferation (p <0.05) and 546 miRs decreased proliferation (p <0.05, Wilcoxon) of NHC3 cells (Fig. 2B). Among pro-proliferative miRs with evaluable phalloidin staining, the majority (66.1%, 361/546) did not affect cell area, suggesting that increased confluency at the final timepoint was not due to epithelial-mesenchymal transition phenotypes. To confirm the pro-proliferative effect of those 548 miRs, two validation screens were subsequently performed in two additional primary NHC models (NHC2 and C324) (Fig. S2B-C). In the validation screens, 326 miRs and 250 miRs were found to significantly increase the proliferation of NHC2 and C324, respectively (Fig. S2D-E). Overall, 179 miR mimics were found to consistently increase proliferation of all three NHC cell models (Fig. 2C; Table S8).

Overlapping the *in vitro* screen results with CCA patient data (Fig. S3A), 39.7% (71/179) miRs were found to be upregulated in patient tumours and to consistently trigger increased proliferation in all cholangiocyte models (Table S9). By using TCGA-CHOL cohort[21] for further validation, this set of fundamental pro-proliferative DEmiRs was refined to five: miR-23a-3p, miR-27a-3p, miR-181-5p, miR-199b-5p, miR-3127-5p (Fig. 2D). To prioritize these miRs for downstream experiments, differential expression and predicted differential activity (inferred from transcriptomic profiles with miReact[22]) of miRs were evaluated. MiR-27a-3p was the only candidate miR whose activity was predicted to be increased in CCA tissues compared to SL and independent normal bile duct samples (Fig. 2E, Fig. S3B). Therefore, miR-27a-3p was selected as the optimal proliferative DEmiR to further characterize *ex vivo*, *in vitro*, and *in vivo*.

MiR-27a-3p affects cell cycle regulation in CCA, involving modulation of FoxO signalling

Integrative analysis of matched miR and transcriptomic data (96 CCA, 58 SL) identified 9,925 genes to be significantly correlated with miR-27a-3p expression (4,382 negatively, 5,543 positively, FDR p <0.05). Pathway over-representation analysis identified 'cell cycle' as the most associated biological process among these genes, a finding that was reproduced in TCGA-CHOL cohort (Fig. 3A, Fig. S4A). To pinpoint which of these genes may be direct targets of this miR, known and/or predicted (minimum eight algorithms) targets whose expression anticorrelated with miR-27a-3p were identified (FDR p <0.05). In total, 263 genes met these criteria and were most significantly over-represented within the FoxO signalling pathway (Fig. 3B, Table S10). MiR-27a-3p targets were also found to be most over-represented among the FoxO signalling pathway in TCGA-CHOL cohort (Fig. S4B). Notably, we found the FoxO signalling pathway to be downregulated in CCA (Fig. 1E) and it is known to be linked to cell cycle regulation in other cancer types.[23] Within the FoxO signalling pathway, miR-27a-3p expression significantly correlated with the expression of 74.1% (80/108) of pathway members in our cohort. These included 12 known targets whose expression inversely correlated with miR-27a-3p (FDR p <0.05) (Fig. 3C). In total, 5 of these candidate miR targets were replicated in TCGA-CHOL cohort: *BNIP3*, *EGFR*, *FOXO1*, *IGF1*, *IRS1* (Table S11). These genes all play distinct roles in the FoxO signalling pathway,

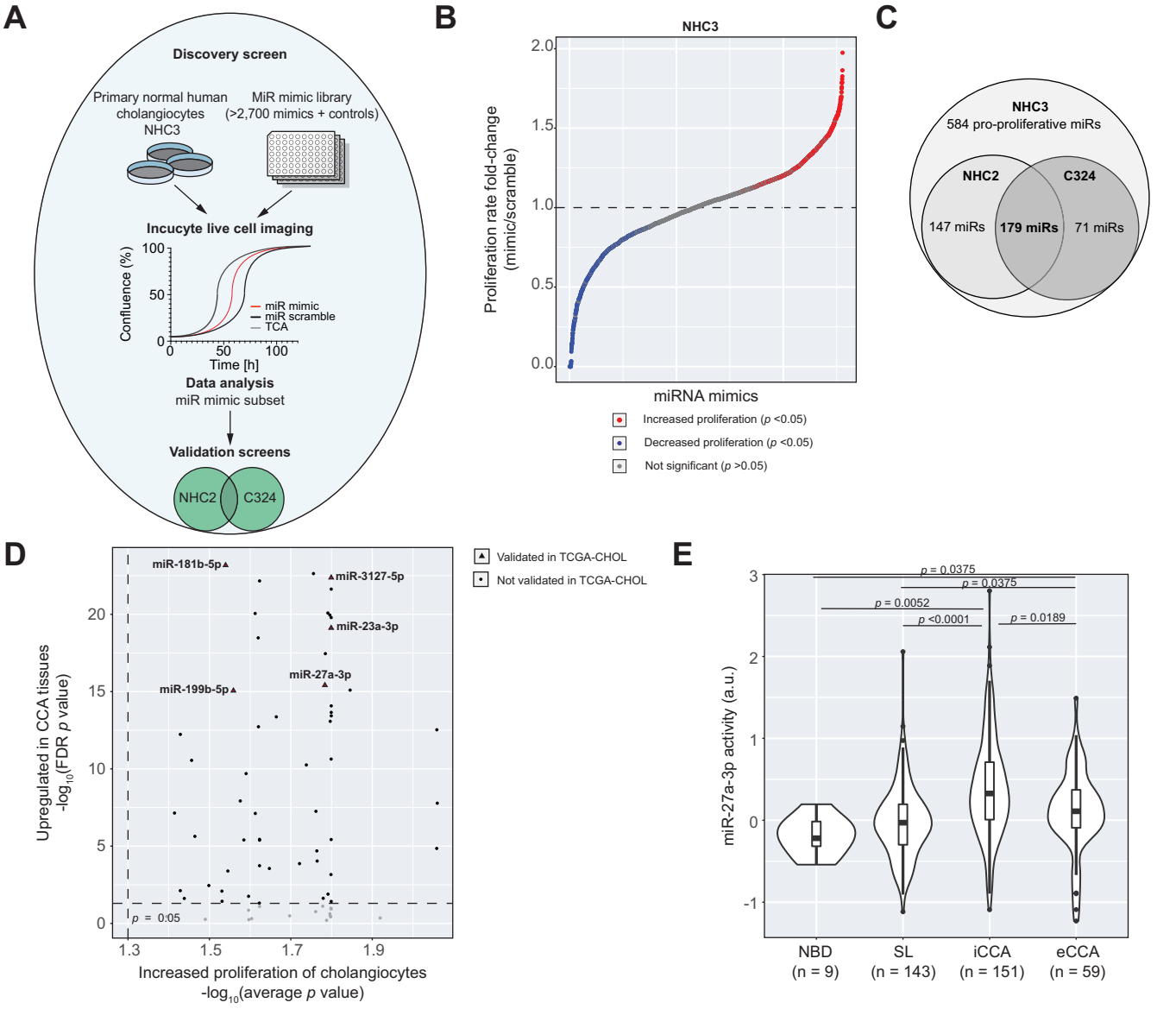

Fig. 2. High-throughput screening of miR mimics in normal human cholangiocytes to identify proliferative miRs. (A) Overview of HTS. (B) S-curve for proliferation effects of miR mimics in the NHC3 culture. 548 miR mimics increased proliferation and 546 mimics decreased proliferation. *p* values were calculated by Wilcoxon rank-sum test. (C) Venn Diagram representing proliferative miRs in the discovery (NHC3) and two validation (NHC2 and C324) screens. (D) Comparison of the expression changes of universal pro-proliferative miRs (HTS) in CCA relative to SL tissues (patients). Highlighted miRs (triangles) were reproducibly differentially expressed in TCGA-CHOL cohort. (E) Violin with boxplots comparing miR-27a-3p activity (estimated by miReact) between NBD (n = 9), SL (n = 143), iCCA (n = 151) and eCCA (n = 59) tissues in our cohort. *p* values were calculated by Wilcoxon rank-sum test. CCA, cholangiocarcinoma; eCCA, extrahepatic CCA; HTS, high-throughput screening; iCCA, intrahepatic CCA; miR, microRNA; NBD, normal bile duct; NHC3, normal human cholangiocyte 3; SL, surrounding liver; TCGA, The Cancer Genome Atlas. (This figure appears in color on the web.)

including signal transduction (*EGFR*, *IGF1*, *IRS1*), transcriptional regulation (*FOXO1*), and autophagy (*BNIP3*) (Fig. 3D).

FOXO1 is a target of miR-27a-3p in cholangiocytes and CCA

In patient tissues, miR-27a-3p was found overexpressed in bulk CCA compared to SL (Fig. 4A) and was expressed in tumour cells as revealed by *in situ* staining (Fig. S5). MiR-27a-3p expression did not differ between small (pT1-2) and large (pT3-4) tumours ($p = 0.12$, Wilcoxon), tumours without (pN0) or with (pN1) lymph node involvement ($p = 0.87$) or based on genomic alterations (Fig. S6A-C). However, high miR-27a-3p expression trended towards an association with decreased patient survival ($p = 0.05$, log-rank) (Fig. S6D). Our *in vitro* CCA cell models (CC16, EGI-1, ETK-1, HuCCT-1) exhibited higher expression of miR-27a-3p compared to primary cholangiocytes (NHC3, miR-seq) (Fig. 4B) and immortalised cholangiocytes (H69, quantitative reverse-transcription PCR [RT-qPCR]) (Fig. 4C). To further characterize the regulatory role(s) of miR-27a-3p, we analysed the five candidate miR-target genes. Only *FOXO1* and its downstream gene *BNIP3* were significantly downregulated at the mRNA level

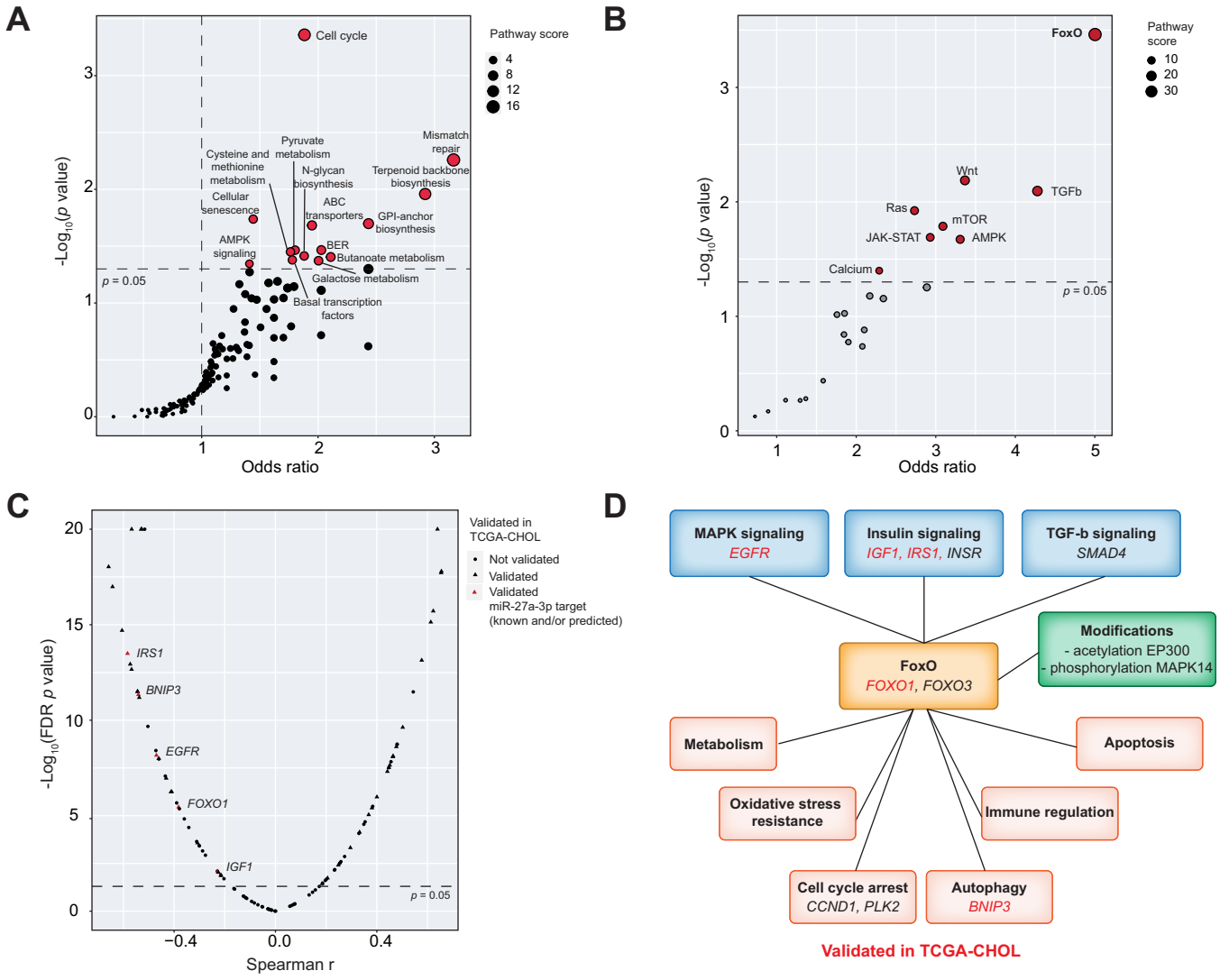

Fig. 3. MiR-27a-3p affects cell cycle regulation in CCA by targeting FoxO signalling. (A) Pathway over-representation analysis of 9,925 genes significantly correlating (Spearman correlation, FDR p <0.05) with miR-27a-3p expression in 96 CCA and 58 SL tissues in our cohort. Pathways were defined by KEGG, analysis was performed using Enrichr, which generated the corresponding statistical metrics (odds ratio, p value, pathway score). (B) Pathway over-representation analysis of 263 genes that are known or predicted (min. 8 algorithms) targets of miR-27a-3p and negatively correlate with miR-27a-3p expression (Spearman correlation, FDR p <0.05) in our cohort. Pathways were defined by KEGG, target prediction was performed with miRWalk. (C) Spearman correlation analysis of miR-27a-3p expression with FoxO signalling pathway members in our cohort. miR-gene expression correlations validated in TCGA-CHOL cohort are triangles. miR-target gene expression correlations validated in TCGA-CHOL cohort are red triangles. Known and/or predicted miR targets are denoted as triangles. miR-target gene expression correlations validated in TCGA-CHOL cohort are highlighted in red. (D) Graphical representation of the biological functions of key miR-27a-3p targets within the FoxO signalling pathway. CCA, cholangiocarcinoma; FDR, false discovery rate; miR, microRNA; SL, surrounding liver; TCGA, The Cancer Genome Atlas. (This figure appears in color on the web.)

in CCA cell lines compared to H69 (Fig. 4D). Thus, the potential interaction between miR-27a-3p and the transcription factor FOXO1, was selected for further evaluation *in vitro*. Reverse-transcription quantitative PCR and immunoblotting confirmed FOXO1 expression to be significantly lower in CCA cells compared to H69 cells (Fig. 4E-F). To confirm the binding of miR-27a-3p to the 3UTR of *FOXO1 in vitro*, a luciferase reporter assay was performed in H69 cells using a wild-type construct and a construct mutated at the candidate miR-27a-3p binding site. After addition of an miR-27a-3p mimic, the luciferase activity level was reduced for the wild-type but not the mutant plasmid, confirming that miR-27a-3p binds to the 3UTR of *FOXO1* and impairs its translation (Fig. 4G).

Knockout of miR-27a-3p affects CCA growth in vitro

To evaluate tumour-associated miR-27a-dependency, CRISPR/Cas9-mediated single-cell knockout of miR-27a in the HuCCT-1 CCA cell line was performed. qRT-PCR confirmed the knockout of miR-27a as part of the miR-23a/27a/24-2 cluster (Fig. 5A, Fig. S7A-B). Knockout of miR-27a in HuCCT-1 led to a significant increase of FOXO1 expression in three independent single-cell knockout clones (Fig. 5B), but only minor changes in upstream miR-27a-targeted FoxO signalling members (Fig. 3D, IRS1, EGFR, IGF-) (Fig. S7C). Comparing knockout clones to wild-type HuCCT-1 cells, loss of miR-27a decreased proliferation and wound healing, as well as impairing colony formation (Fig. 5C-F), whereas an unsuccessful

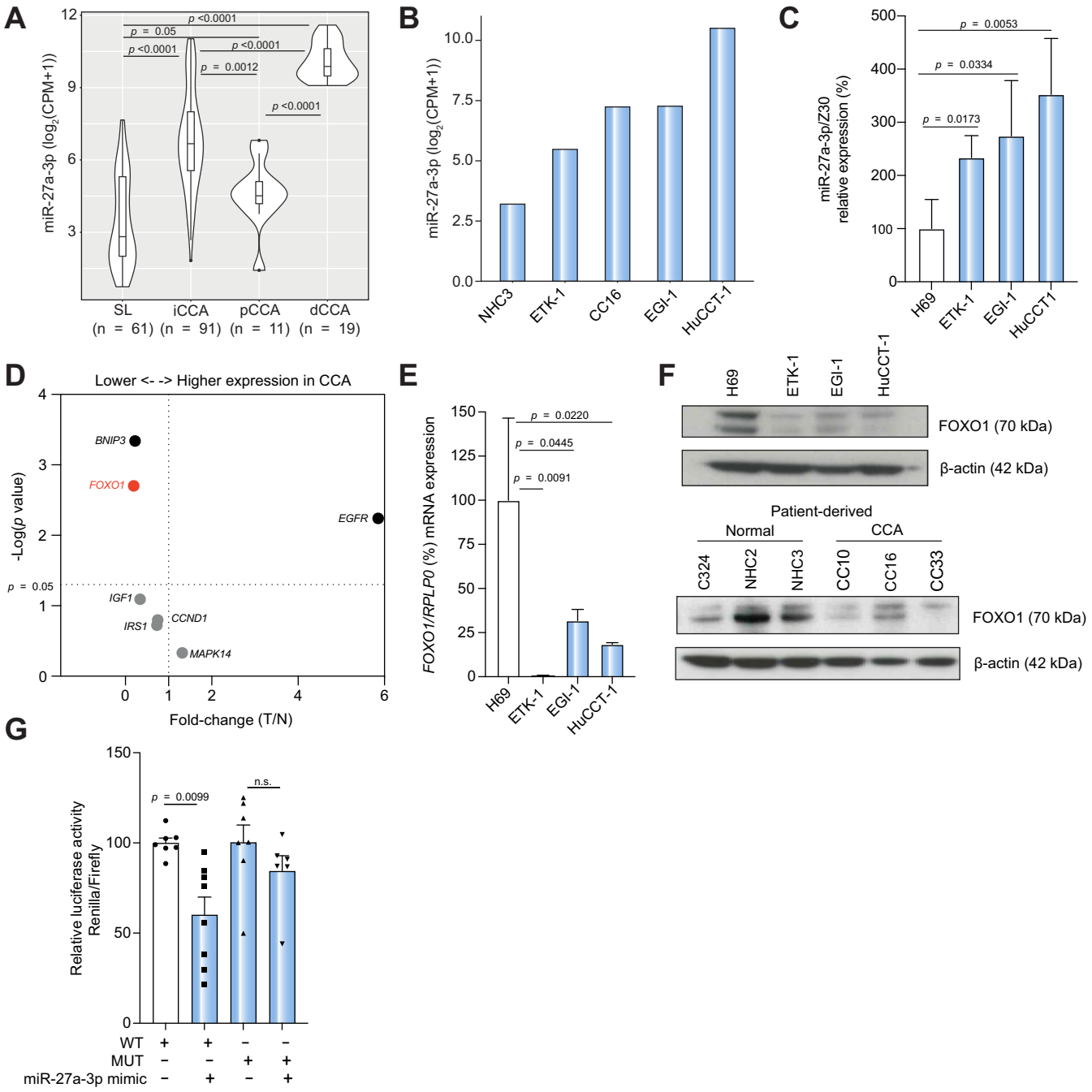

Fig. 4. FoxO signalling is deregulated by miR-27a-3p through interaction with *FOXO1*. (A) Differential expression of miR-27a-3p (small RNAseq) between SL (n = 61), iCCA (n = 91), pCCA (n = 11) and dCCA (n = 19) in our cohort. *p* values were calculated by Wilcoxon rank-sum test. (B) Differential expression of miR-27a-3p (small RNAseq) between primary normal cholangiocytes (NHC3) and CCA (CC16, EGI-1, HuCCT-1, ETK-1) cell lines. (C) Differential expression of miR-27a-3p (qRT-PCR) between immortalised cholangiocyte (H69) and CCA (CC16, EGI-1, HuCCT-1, ETK-1) cell lines. Z30 was used as an endogenous housekeeping gene. *p* values were calculated by unpaired *t* test. (D) Fold-change of expression levels between tumour (T, n = 21) and non-tumour cell lines (N, n = 7) of selected 7 genes, which are known/predicted miR-27a-3p target genes with negative correlation in our cohort and TCGA-CHOL. (E) Differential expression of *FOXO1* mRNA by qRT-PCR between immortalised cholangiocytes (H69) and CCA (EGI-1, HuCCT-1, ETK-1) cell lines. *RPLP0* was used as an endogenous housekeeping gene. *p* values were calculated by unpaired *t* test. (F) Immunoblot of FOXO1 expression in cholangiocytes (C324, H69, NHC2, NHC3) and CCA cell lines (EGI-1, HuCCT-1, ETK-1). β-actin was used as a loading control. (G) Luciferase assay with *FOXO1* 3UTR WT and MUT plasmids were performed in combination with and without miR-27a-3p mimic transfection. Renilla luminescence was normalized to Firefly luciferase activity. *p* values were calculated by one-way ANOVA (n = 6, n.s. *p* >0.05). CCA, cholangiocarcinoma; dCCA, distal CCA; iCCA, intrahepatic CCA; miR, microRNA; MUT, miR-27a-3p binding mutant; NHC3, normal human cholangiocyte 3; pCCA, perihilar CCA; qRT-PCR, quantitative reverse-transcription PCR; WT, wild-type. (This figure appears in color on the web.)

CRISPR/Cas9 clone (WT clone) without changes in miR-27a-3p expression by qRT-PCR showed no significant phenotypic changes compared to HuCCT-1 (Fig. S7D-F). MiR-27a knockout-associated FOXO1 upregulation and associated phenotypes were further confirmed in the CCA cell line, ETK-1 (Fig. S7G-J). As FOXO1 is a key regulator of metabolism, we

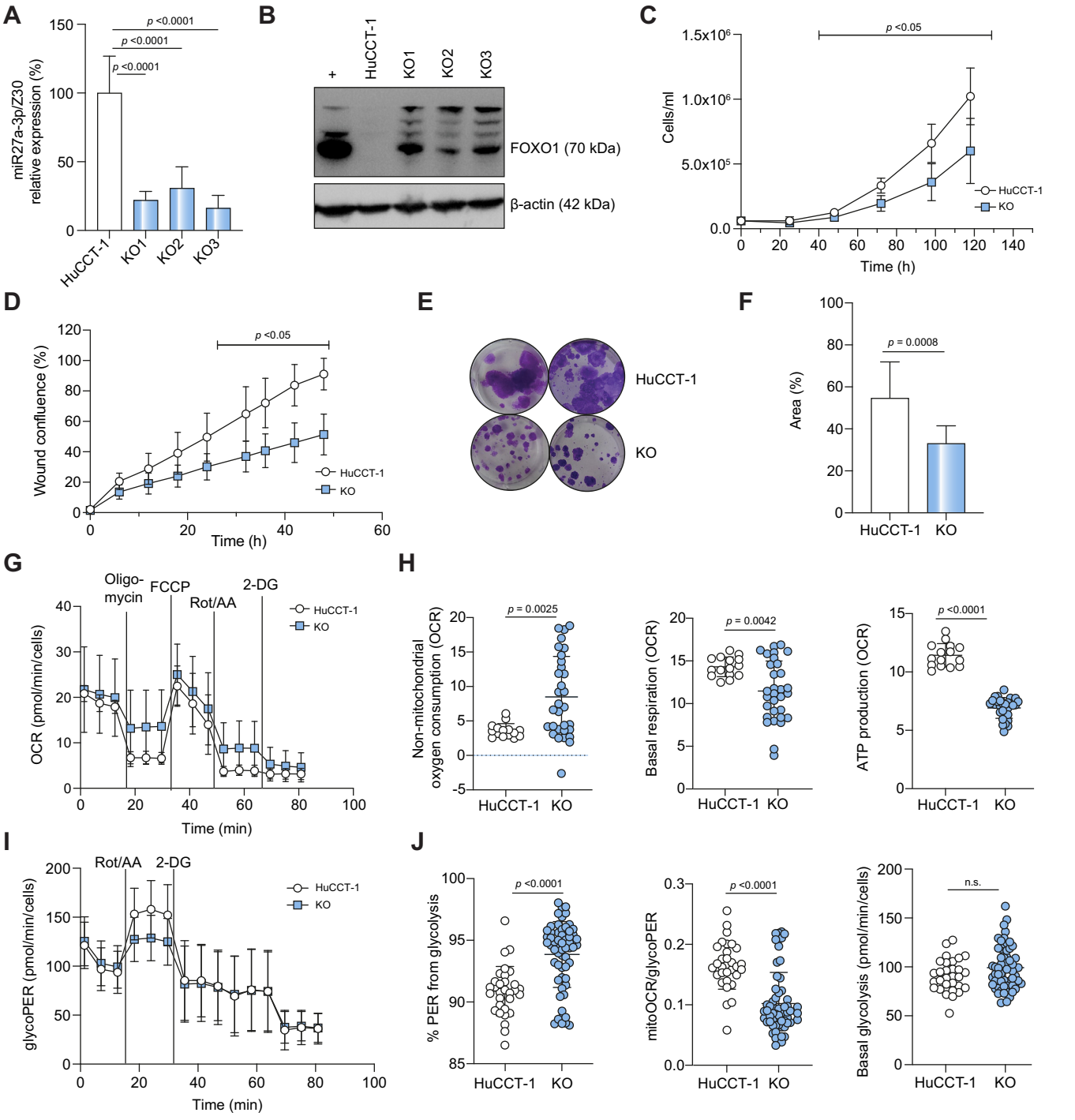

Fig. 5. MiR-27a knockout affects CCA proliferation, migration and colony formation *in vitro*. (A) Differential expression of miR-27a-3p in three independent single-cell knockout clones generated by CRISPR/Cas9 nickase. *p* values were calculated by unpaired *t* test. (B) Western blot for FOXO1 in miR-27a CRISPR/Cas9 knockout clones. β-actin expression was used as control. (C) Proliferation (cell count) of HuCCT-1 miR-27a knockouts in three independent biological replicas compared to wild-type. *p* values were calculated by non-parametric two-way ANOVA. (D) Wound healing ability (IncuCyte) of HuCCT-1 miR-27a knockouts compared to wild-type in three independent runs. *p* values were calculated by non-parametric two-way ANOVA. (E-F) Representative image (E) and quantification (F) of the clonogenicity (colony formation assay) of HuCCT-1 miR-27a knockouts compared to wild-type in three independent runs. Cell surface area was quantified with ImageJ. *p* values were calculated by non-parametric two-way ANOVA. (G-H) Representation of the following mitochondrial function parameters: OCR (G), non-mitochondrial oxygen consumption, basal respiration, and ATP production (H) based on Seahorse Mito Stress Test. *p* values were calculated by Mann-Whitney test. (I-J) Representation of the following glycolytic rate parameters: glycolytic proton efflux rate (glycoPER, I), %PER from glycolysis, mitochondrialOCR/glycoPER and basal glycolysis (J) based on Seahorse Glycolytic Rate Test. *p* values were calculated by Mann-Whitney test. 2-DG, 2-deoxy-D-glucose; CCA, cholangiocarcinoma; FCCP, carbonyl cyanide-4-(trifluoromethoxy) phenylhydrazone; KO, knockout; miR, microRNA; OCR, oxygen consumption rate; Rot/AA, rotenone/antimycin A; (This figure appears in color on the web.)

examined the mitochondrial function and glycolytic rate in HuCCT-1 and miR-27a knockout (KO1 and KO3) by Seahorse Cell Mito Stress and glycolytic rate test (Fig. 5G-J, Fig. S8). We observed a reduction of non-mitochondrial oxygen consumption, in combination with decreased basal respiration and ATP production (Fig. 5H), indicating reduced mitochondrial function following miR-27a knockout. The reduction in mitochondrial activity is accompanied by an increased dependence on glycolysis, as shown by % proton efflux rate and the ratio between mitochondrial oxygen consumption rate and glycolytic proton efflux rate (Fig. 5I-J). Nevertheless, basal glycolysis and the glycolysis product L-lactic acid (Fig. 5J, Fig. S8H) remain unchanged, suggesting a reduced glycolytic efficiency in miR-27a knockout compared to wild-type CCA cells.

MiR-27a knockout impedes tumour growth and proliferation in vivo

To determine the consequences of miR-27a knockout on tumour proliferation *in vivo*, two miR-27a knockout clones were chosen for subcutaneous injection (KO1 and KO3). No significant difference in cell viability (WST-1) was found between the knockout clones and wild-type cells prior to transplantation (Fig. S9A). After injection of tumour cells, the palpable growth rate of knockout and wild-type (HuCCT-1) tumours separated after 25 days (Fig. S9A). Overall, miR-27a knockout cells gave rise to smaller tumours (size) and lower tumour weights (p = 0.0026 for KO1 and p = 0.0041 for KO2) at the study endpoint (34 days) compared to wild-type (Fig. 6A-B). Histopathological evaluation indicated that the tumours did not differ in differentiation grade (grade 3) or necrosis between wild-type and knockout models (Fig. 6C). However, based on HE stains, knockout tumours demonstrated a greater abundance of clear cytoplasm content, less fibrous stromal reaction and lower collagen deposition. Conversely, wild-type tumours were characterized by greater eosinophilic cytoplasm content, more severe fibrous stroma, and more hyaline tissue (Fig. 6C). qRT-PCR analysis and immunofluorescence staining of the tumour tissues confirmed significantly lower expression of miR-27a-3p and higher nuclear expression of FOXO1 in knockout cells, in association with lower levels of the proliferation marker, Ki67 (Fig. 6D-E, Fig. S9C-D).

Discussion

Limited miR profiling studies have been conducted in individuals with CCA, though they have typically been characterized by modest-to-small sample sizes, use of microarrays with pre-specified miR probes, and lack of matching transcriptome or functional data.[11,21,24] Herein, we characterised

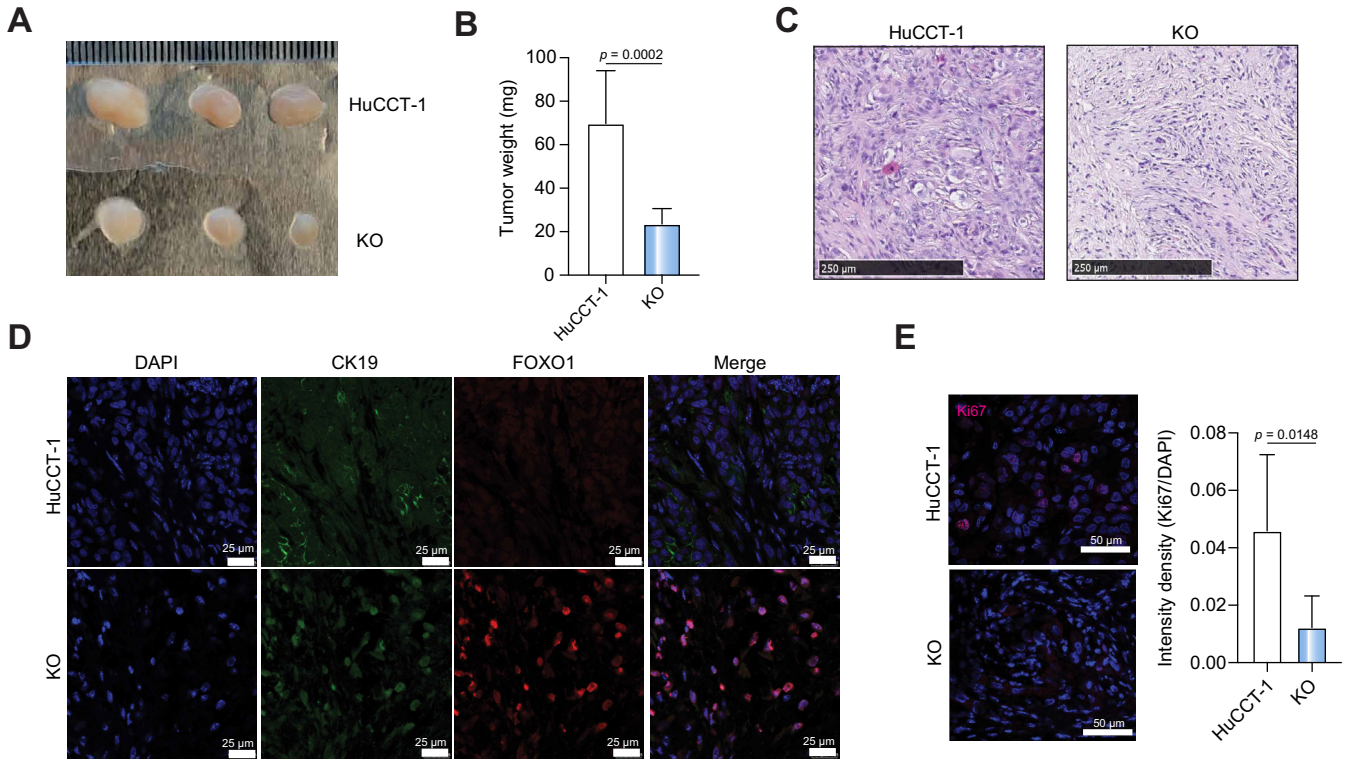

Fig. 6. MiR-27a knockout impedes tumour growth in association with FOXO1 upregulation. (A) Representative images of tumour size at study endpoint after subcutaneous xenograft of miR-27a knockout clones (KO) and wild-type HuCCT-1 into mice. (B) Tumour weights at study endpoint. p values were calculated by unpaired t test. (C) H&E stains of xenograft tumour tissues derived from miR-27a knockout clones and wild-type HuCCT-1. (D) Immunofluorescence of tumour tissue confirms upregulation of FOXO1 expression in miR-27a knockout clones compared to HuCCT-1 wild-type. Cancer cells were labelled with the cholangiocyte marker CK19 and DAPI counterstain. (Leica SP8, 63x oil objective). (E) Immunofluorescence of Ki67 proliferation marker in HuCCT-1 wild-type (n = 4) and knockout tumour tissue (n = 4) of mouse xenograft. The nucleus of the cells was counterstained by DAPI. (Leica SP8, 63x oil objective). The intensity density of Ki67 signal was quantified in two independent frames of each tumour and was normalized to DAPI stain. After identification of outliers by ROUT method, p values were calculated by unpaired t test. KO, miR-27a knockout clones; miR, microRNA. (This figure appears in color on the web.)

the miR profiles of a comparatively large cohort (119 CCA, 63 SL) using unbiased small RNAseq, among which matched transcriptome data were available for 84.6% (154/182) of samples. Our observation that 96.4% (135/140) of DEmiRs are upregulated in tumours suggests predominantly oncogenic roles of miRs through inhibition of tumour suppressors in CCA, which has also been reported in a previous pan-cancer study.[25] MiRs regulate the transcriptome by repressing translation or inducing the degradation of their target mRNAs. It is estimated that each miR family targets around 450 mRNAs, and transcriptome regulation is primarily executed by targeting transcription factors.[26,27] However, selection of target mRNAs is highly context-specific and sensitive to the relative abundance of target mRNA, implicating these non-coding regulators in inter- and intra-tumour heterogeneity. By performing a parallel proliferation screen using miR mimics in primary cholangiocytes, we identified a compendium of pro-proliferative miRs in CCA, and further characterized the impact of miR-27a-3p on FoxO signalling through its transcription factor target, FOXO1.

Epigenetic deregulation, especially aberrant expression of miRs, is initiated in pro-inflammatory states and pre-invasive lesions of CCA.[28] Inflammation and increases in interleukin (IL)-6 expression are known to induce proliferation of normal cholangiocytes and are therefore linked to hyperplasia and CCA development,[29–31] which is at least partially regulated through the action of miRs. In cholestatic rats, downregulation of miR-124 leads to increased expression of IL-6R and STAT3 inducing IL-6-mediated proliferation of cholangiocytes.[29] Additionally, pro-inflammatory cytokines (IL-8, IL-12, IL-18) induce the expression of miR-506 and miR-425 in cholangiocytes, further enhancing inflammation by increasing the expression of inflammatory markers and cytokine production.[32,33] To date, two studies have characterized progressive miR expression alterations in the development of CCA from hyperplasia, highlighting their essential role in disease initiation and development.[34,35]

Our miR mimic screen uncovered proliferative roles for 52.6% (71/135) of patient DEmiRs in normal human cholangiocytes lacking genetic or chemical insults, indicating that a majority of these miRs are functional in cholangiocytes and could potentially contribute to ductular reaction in response to liver injury. However, these DEmiRs also likely include “miR tumour-dependencies” that become important for tumour cell survival, as well as miRs that predominantly exert their pro-tumourigenic effects following extravesicular-mediated trafficking from epithelia to cells of the microenvironment. Therefore, the extent to which miRs can malignify cholangiocytes independently of genomic alterations and cells of the microenvironment remains unresolved. The timing of these miR aberrations during cholangiocarcinogenesis might provide some clues as to their cholangiocyte-intrinsic functions during transformation. Therefore, evaluation of miR dynamics in multiregional and/or longitudinally sampled tissues representative of disease evolution (normal bile duct, ductular reaction, carcinoma *in situ*, invasive CCA) is warranted.

We have observed miR-mediated suppression of FoxO signalling in CCA, indicating a tumour-inhibitory function of the pathway. The FoxO family (FOXO1, FOXO3A, FOXO4 and FOXO6) is a known tumour suppressive family controlling the transcription of genes involved in cell cycle arrest, apoptosis, autophagy, anti-oxidative enzymes, metabolism, and immune regulators.[23,36] Thus, for cellular homeostasis, tight regulation of the abundance of FoxO family members by post-transcriptional and -translational regulation is essential. In CCA, little is known about the FoxO transcription factor family, with only FOXO3 having been studied so far. FOXO3 downregulation and phosphorylation-associated inactivation due to constitutively active Akt contributed to cisplatin resistance in CCA.[37] Phosphorylation of FOXO1 leads to sequestering of the protein in the cytoplasm, thereby inhibiting the transcription of FOXO1 target genes. In contrast, dephosphorylated FOXO1 is located in the nuclei, ensuring active transcription. We have shown that FOXO1 is regulated by miR-27a-3p in CCA, impairing mitochondrial function and resulting in a nuclear localization of FOXO1 in miR-27a knockout mouse tumours, which indicates its transcriptionally active dephosphorylated status. FOXO1 promotes cell viability and decreased apoptosis in HCC,[38,39] contributes to mitochondrial dysfunction and reduction of proliferation in endothelial cells[40] and regulates glycolysis in macrophages,[41] supporting the phenotype observed in CCA. How FOXO1 functions as a tumour suppressor in CCA requires further elucidation by identifying its transcriptional target genes by combined RNAseq and chromatin immunoprecipitation-sequencing analyses.

Several limitations apply to our study. While we decided to focus on the proliferative roles of miRs in CCA, miRs contribute to diverse hallmarks of tumour biology that are independent of proliferation and are therefore not assessed by our *in vitro* screen. As strategies for miR inhibition like miRZip or locked-nucleic acids only introduce transient knockdown effects and are not suitable for long-term experiments, such as *in vivo* studies, we applied CRISPR/Cas9nickase editing to knockout miR-27a. Though successful, we observed a reduction of the whole miR-23a/27a/24-2 cluster as editing may have led to impaired maturation of all miRs in the miR stem loop; thus, it is not possible to completely uncouple our observed phenotypes from the contribution of other family members. While our study is the largest miR study reported in CCA to date, this mixed cohort is still relatively small to define specific roles for miRs in tumour anatomical subgroups. This may be particularly important given the substantial differences in DEmiRs between tumour anatomical subgroups in our study, as well as the increasing divergence of treatment strategies for individuals with intrahepatic and extrahepatic CCA. Other stratification approaches are gaining clinical and biological traction (histological variants, morphological growth patterns) and future analysis of miR heterogeneity may benefit from considering these classifications. Finally, although miR delivery methods are constantly improving, the cellular- and context-specific activity of miRs make it challenging to target them therapeutically.[42] Identifying synthetic lethality interactions of miRs (*i.e.*, tumour survival co-dependencies on proteins more amenable to therapeutic development) could provide a possible solution in the future.

In conclusion, we have characterized the aberrant miRNomes of CCA tissues, including their consequences for transcriptome homeostasis and transcription factor regulation. Our results suggest that CCA-associated miRs induce hyperproliferation of normal cholangiocytes, potentially contributing to cholangiocarcinogenesis. Furthermore, our targeted analysis

of miR-27a-3p implicate this oncogenic miR in cell cycle regulation via the FoxO signalling pathway, rendering miR-27a-3p a tumour dependency *in vitro* and *in vivo*. Collectively, these data implicate miRNA-mediated transcription factor regulation in the expansive transcriptome reprogramming characteristic of CCA.

Affiliations

[1]Biotech Research & Innovation Centre (BRIC), Department of Health and Medical Sciences, University of Copenhagen, Ole Maaløes Vej 5, 2200, Copenhagen N, Denmark; [2]Department of Oncology, Herlev and Gentofte Hospital, Copenhagen University Hospital, Herlev, Denmark; [3]Bioneer, Kogle Alle 2, DK-2970, Hørsholm, Denmark; [4]Institute of Medical Genetics and Pathology, University Hospital Basel, Basel, Switzerland; [5]Department of Liver and Gastrointestinal Diseases, Biodonostia Health Research Institute, Donostia University Hospital, University of the Basque Country (UPV/EHU), San Sebastian, Spain; [6]National Institute for the Study of Liver and Gastrointestinal Diseases (CIBERehd, "Instituto de Salud Carlos III"), Spain; [7]IKERBASQUE, Basque Foundation for Science, Bilbao, Spain; [8]Department of Biochemistry and Genetics, School of Sciences, University of Navarra, Pamplona, Spain; [9]Department of Drug Design and Pharmacology, Faculty of Health and Medical Sciences, University of Copenhagen, Denmark; [10]Department of Epidemiology, Shanghai Cancer Institute, Shanghai, China; [11]Department of Medicine I, University Medical Center Schleswig-Holstein-Campus Lübeck, 23558 Lübeck, Germany; [12]Division of Gastroenterology and Hepatology, Mayo Clinic College of Medicine, Rochester, MN, USA; [13]Coimbra Institute for Clinical and Biomedical Research (iCBR) Area of Environment, Genetics and Oncobiology (CIMAGO), Institute of Biophysics, Faculty of Medicine, University of Coimbra, Portugal; [14]Centro Hospitalar e Universitário de Coimbra, Coimbra, Portugal; [15]Division of Cancer Epidemiology and Genetics, NIH, USA

Abbreviations

CCA, cholangiocarcinoma; DEmiRs, differentially expressed miRs; FDR, false discovery rate; FoxO, forkhead box O family; IL-, interleukin-; KO, miR-27a knockout clones; miR, microRNA; RT-qPCR, quantitative reverse-transcription PCR; SL, surrounding liver; RNAseq, RNA sequencing; TCGA, The Cancer Genome Atlas; WT, wild-type.

Financial support

The Laboratory of JBA is funded by a competitive grant from the Novo Nordisk Foundation (#14040). PMG, CJO, JFLB were awarded postdoc fellowships from the European Union Marie Curie program – MiRCHOL, EpiTarget and EpiCC, respectively. PMG was awarded a Sheila Sherlock postdoc fellowship from the European Association for the Study of the Liver (EASL). AT was awarded an individual postdoc fellowship from the Lundbeck Foundation. LD was awarded a PhD project grant from the Danish Cancer Research Foundation. This project was supported by the European Union's Horizon 2020 research and innovation program under the Marie Skłodowska-Curie grant agreement no. 801481. JMB is supported by Spanish Carlos III Health Institute (ISCIII) [(FIS PI18/01075, PI21/00922, and Miguel Servet Programme CPII19/00008) cofinanced by "Fondo Europeo de Desarrollo Regional" (FEDER)] and CIBERehd (ISCIII); La Caixa Scientific Foundation (HR17-00601); AMMF-The Cholangiocarcinoma Charity (EU/2019/AMMFt/001); PSC Partners US and PSC Supports UK (06119JB); European Union's Horizon 2020 Research and Innovation Program [grant number 825510, ESCALON]. MSM is supported by the National Science Foundation (SNSF; Grant No. 320030_189275)

Conflicts of interest

JBA is a member of the scientific advisory board at SEALD, Norway and reports scientific consultancies for QED Therapeutics and Flagship Pioneering. JBA has received funding from Incyte. MSM has served as a consultant for Novartis and GSK, and received speaker honoraria from ThermoFisher and Merck, all outside the current work.

Please refer to the accompanying ICMJE disclosure forms for further details.

Authors' contributions

JBA, PMG, CJO, LD conceived the idea, designed and implemented the study; LD, PMG, CJO, ML, RCO, JLFB, LS, DH, AT, BIA, BSN, AG performed experiments and data analyses; LD, PMG, CJO, JBA interpreted omics data; JBA, LRR, RCO, JK, YTG, JUM, JMB, MSM patient recruitment, clinical data collection and pathological assessment; LD, CJO, PMG, JBA wrote the manuscript; all authors read, edited and approved the manuscript.

Data availability statement

Whole-transcriptome profiling and miR sequencing data can be made available upon request following IRB approval.

Acknowledgements

The authors would like to thank members of the Biotech Research and Innovation Centre (BRIC) Histocore, Microscopy and High Throughput robotics screening facilities. The project described was supported in parts by Award Number P50 CA210964 (Mayo Clinic Hepatobiliary SPORE) from the National Cancer Institute (NCI), USA. The content is solely the responsibility of the authors and does not necessarily represent the official views of the NIH, USA. Furthermore, the results are in part supported by data generated by the TCGA Research Network: https://www.cancer.gov/tcga.

Supplementary data

Supplementary data to this article can be found online at https://doi.org/10.1016/j.jhep.2022.10.012.

References

Author names in bold designate shared co-first authorship

[1] Banales JM, Marin JJG, Lamarca A, Rodrigues PM, Khan SA, Roberts LR, et al. Cholangiocarcinoma 2020: the next horizon in mechanisms and management. Nat Rev Gastroenterol Hepatol 2020;17(9):557–588.

[2] Izquierdo-Sanchez L, Lamarca A, La Casta A, Buettner S, Utpatel K, Klumpen HJ, et al. Cholangiocarcinoma landscape in Europe: diagnostic, prognostic and therapeutic insights from the ENSCCA Registry. J Hepatol 2022 May;76(5):1109–1121.

[3] **Hogdall D**, **Lewinska M**, Andersen JB. Desmoplastic tumor microenvironment and immunotherapy in cholangiocarcinoma. Trends Cancer 2018;4(3):239–255.

[4] **Del Poggetto E**, **Ho IL**, Balestrieri C, Yen EY, Zhang S, Citron F, et al. Epithelial memory of inflammation limits tissue damage while promoting pancreatic tumorigenesis. Science 2021;373(6561):eabj0486.

[5] Nakamura H, Arai Y, Totoki Y, Shirota T, Elzawahry A, Kato M, et al. Genomic spectra of biliary tract cancer. Nat Genet 2015;47(9):1003–1010.

[6] **Wardell CP**, **Fujita M**, Yamada T, Simbolo M, Fassan M, Karlic R, et al. Genomic characterization of biliary tract cancers identifies driver genes and predisposing mutations. J Hepatol 2018;68(5):959–969.

[7] **Nepal C**, **O'Rourke CJ**, Oliveira D, Taranta A, Shema S, Gautam P, et al. Genomic perturbations reveal distinct regulatory networks in intrahepatic cholangiocarcinoma. Hepatology 2018;68(3):949–963.

[8] Consortium ITP-CAoWG. Pan-cancer analysis of whole genomes. Nature 2020;578(7793):82–93.

[9] **Jusakul A**, **Cutcutache I**, **Yong CH**, **Lim JQ**, Huang MN, Padmanabhan N, et al. Whole-genome and epigenomic landscapes of etiologically distinct subtypes of cholangiocarcinoma. Cancer Discov 2017;7(10):1116–1135.

[10] O'Rourke CJ, Lafuente-Barquero J, Andersen JB. Epigenome remodeling in cholangiocarcinoma. Trends Cancer 2019;5(6):335–350.

[11] Oishi N, Kumar MR, Roessler S, Ji J, Forgues M, Budhu A, et al. Transcriptomic profiling reveals hepatic stem-like gene signatures and interplay of miR-200c and epithelial-mesenchymal transition in intrahepatic cholangiocarcinoma. Hepatology 2012;56(5):1792–1803.

[12] Salati M, Braconi C. Noncoding RNA in cholangiocarcinoma. Semin Liver Dis 2019;39(1):13–25.

[13] **Liu CH**, **Huang Q**, Jin ZY, Zhu CL, Liu Z, Wang C. miR-21 and KLF4 jointly augment epithelialmesenchymal transition via the Akt/ERK1/2 pathway. Int J Oncol 2017;50(4):1109–1115.

[14] Wang LJ, He CC, Sui X, Cai MJ, Zhou CY, Ma JL, et al. MiR-21 promotes intrahepatic cholangiocarcinoma proliferation and growth in vitro and in vivo by targeting PTPN14 and PTEN. Oncotarget 2015;6(8):5932–5946.

[15] Lampis A, Carotenuto P, Vlachogiannis G, Cascione L, Hedayat S, Burke R, et al. MIR21 drives resistance to heat shock protein 90 inhibition in cholangiocarcinoma. Gastroenterology 2018;154(4):1066–10679 e5.

[16] Andersen JB, Spee B, Blechacz BR, Avital I, Komuta M, Barbour A, et al. Genomic and genetic characterization of cholangiocarcinoma identifies therapeutic targets for tyrosine kinase inhibitors. Gastroenterology 2012;142(4):1021–1031 e15.
[17] Castven D, Becker D, Czauderna C, Wilhelm D, Andersen JB, Strand S, et al. Application of patient-derived liver cancer cells for phenotypic characterization and therapeutic target identification. Int J Cancer 2019;144(11):2782–2794.
[18] Munoz-Garrido P, Marin JJ, Perugorria MJ, Urribarri AD, Erice O, Saez E, et al. Ursodeoxycholic acid inhibits hepatic cystogenesis in experimental models of polycystic liver disease. J Hepatol 2015;63(4):952–961.
[19] Merino-Azpitarte M, Lozano E, Perugorria MJ, Esparza-Baquer A, Erice O, Santos-Laso A, et al. SOX17 regulates cholangiocyte differentiation and acts as a tumor suppressor in cholangiocarcinoma. J Hepatol 2017;67(1):72–83.
[20] O'Rourke CJ, Matter MS, Nepal C, Caetano-Oliveira R, Ton PT, Factor VM, et al. Identification of a pan-gamma-secretase inhibitor response signature for notch-driven cholangiocarcinoma. Hepatology 2020;71(1):196–213.
[21] Farshidfar F, Zheng S, Gingras MC, Newton Y, Shih J, Robertson AG, et al. Integrative genomic analysis of cholangiocarcinoma identifies distinct IDH-mutant molecular profiles. Cell Rep 2017;19(13):2878–2880.
[22] Nielsen MM, Pedersen JS. miRNA activity inferred from single cell mRNA expression. Sci Rep 2021;11(1):9170.
[23] Xing YQ, Li A, Yang Y, Li XX, Zhang LN, Guo HC. The regulation of FOXO1 and its role in disease progression. Life Sci 2018;193:124–131.
[24] Loeffler MA, Hu J, Kirchner M, Wei X, Xiao Y, Albrecht T, et al. miRNA profiling of biliary intraepithelial neoplasia reveals stepwise tumorigenesis in distal cholangiocarcinoma via the miR-451a/ATF2 axis. J Pathol 2020;252(3):239–251.
[25] Dhawan A, Scott JG, Harris AL, Buffa FM. Pan-cancer characterisation of microRNA across cancer hallmarks reveals microRNA-mediated downregulation of tumour suppressors. Nat Commun 2018;9(1):5228.
[26] Friedman RC, Farh KK, Burge CB, Bartel DP. Most mammalian mRNAs are conserved targets of microRNAs. Genome Res 2009;19(1):92–105.
[27] **Gosline SJ**, **Gurtan AM**, JnBaptiste CK, Bosson A, Milani P, Dalin S, et al. Elucidating MicroRNA regulatory networks using transcriptional, post-transcriptional, and histone modification measurements. Cell Rep 2016;14(2):310–319.
[28] Goeppert B, Stichel D, Toth R, Fritzsche S, Loeffler MA, Schlitter AM, et al. Integrative analysis reveals early and distinct genetic and epigenetic changes in intraductal papillary and tubulopapillary cholangiocarcinogenesis. Gut 2022 Feb;71(2):391–401.
[29] Xiao Y, Wang J, Yan W, Zhou Y, Chen Y, Zhou K, et al. Dysregulated miR-124 and miR-200 expression contribute to cholangiocyte proliferation in the cholestatic liver by targeting IL-6/STAT3 signalling. J Hepatol 2015;62(4):889–896.
[30] Isomoto H, Kobayashi S, Werneburg NW, Bronk SF, Guicciardi ME, Frank DA, et al. Interleukin 6 upregulates myeloid cell leukemia-1 expression through a STAT3 pathway in cholangiocarcinoma cells. Hepatology 2005;42(6):1329–1338.
[31] Wehbe H, Henson R, Meng F, Mize-Berge J, Patel T. Interleukin-6 contributes to growth in cholangiocarcinoma cells by aberrant promoter methylation and gene expression. Cancer Res 2006;66(21):10517–10524.
[32] **Erice O**, **Munoz-Garrido P**, Vaquero J, Perugorria MJ, Fernandez-Barrena MG, Saez E, et al. MicroRNA-506 promotes primary biliary cholangitis-like features in cholangiocytes and immune activation. Hepatology 2018;67(4):1420–1440.
[33] Nakagawa R, Muroyama R, Saeki C, Goto K, Kaise Y, Koike K, et al. miR-425 regulates inflammatory cytokine production in CD4(+) T cells via N-Ras upregulation in primary biliary cholangitis. J Hepatol 2017;66(6):1223–1230.
[34] Montal R, Sia D, Montironi C, Leow WQ, Esteban-Fabro R, Pinyol R, et al. Molecular classification and therapeutic targets in extrahepatic cholangiocarcinoma. J Hepatol 2020;73(2):315–327.
[35] Sia D, Hoshida Y, Villanueva A, Roayaie S, Ferrer J, Tabak B, et al. Integrative molecular analysis of intrahepatic cholangiocarcinoma reveals 2 classes that have different outcomes. Gastroenterology 2013;144(4):829–840.
[36] Accili D, Arden KC. FoxOs at the crossroads of cellular metabolism, differentiation, and transformation. Cell 2004;117(4):421–426.
[37] Guan L, Zhang L, Gong Z, Hou X, Xu Y, Feng X, et al. FoxO3 inactivation promotes human cholangiocarcinoma tumorigenesis and chemoresistance through Keap1-Nrf2 signaling. Hepatology 2016;63(6):1914–1927.
[38] Yang XW, Shen GZ, Cao LQ, Jiang XF, Peng HP, Shen G, et al. MicroRNA-1269 promotes proliferation in human hepatocellular carcinoma via down-regulation of FOXO1. BMC Cancer 2014;14:909.
[39] Yang L, Peng F, Qin J, Zhou H, Wang B. Downregulation of microRNA-196a inhibits human liver cancer cell proliferation and invasion by targeting FOXO1. Oncol Rep 2017;38(4):2148–2154.
[40] Wilhelm K, Happel K, Eelen G, Schoors S, Oellerich MF, Lim R, et al. FOXO1 couples metabolic activity and growth state in the vascular endothelium. Nature 2016;529(7585):216–220.
[41] Yan K, Da TT, Bian ZH, He Y, Liu MC, Liu QZ, et al. Multi-omics analysis identifies FoxO1 as a regulator of macrophage function through metabolic reprogramming. Cell Death Dis 2020;11(9):800.
[42] **Chakraborty C**, **Sharma AR**, Sharma G, Lee SS. Therapeutic advances of miRNAs: a preclinical and clinical update. J Adv Res 2021;28:127–138.